
Temperature Dependence of the First-Order Raman Phonon Lines in $\text{GaS}_{0.25}\text{Se}_{0.75}$ Layered Crystals

N.M. GASANLY*

Department of Physics, Middle East Technical University, 06531 Ankara, Turkey

(Received July 4, 2002; in final form September 24, 2002)

Systematic measurements by Raman scattering of the frequency and line width of the zone-center optical modes in $\text{GaS}_{0.25}\text{Se}_{0.75}$ layered crystal over the temperature range of 10–300 K are carried out. The analysis of temperature dependence of intralayer modes shows that frequency shift and line broadening are successfully modeled by including the contributions from thermal expansion and lattice anharmonicity. The purely anharmonic contribution (phonon–phonon coupling) is found to be due to three-phonon processes.

PACS numbers: 78.20.-e, 78.30.-j, 78.30.Hv

1. Introduction

GaS and GaSe semiconducting compounds crystallize in a layered structure. These layered crystals are characterized by highly anisotropic bonding forces. The high anisotropy arises from the fact that the bonding within the layers is considerably stronger than that perpendicular to them. In these compounds, van der Waals forces contribute predominantly to the interlayer interaction, while the bonding forces within the layers are ionic-covalent. The layered compounds GaS and GaSe form a continuous series of $\text{GaS}_{1-x}\text{Se}_x$ mixed crystals ($0 \leq x \leq 1$) [1, 2].

Raman spectroscopy is a powerful technique for obtaining information on various vibrational modes in crystals. The frequency and line width of the phonon lines in the light scattering spectra depend on the crystal temperature. The shift

*e-mail: nizami@metu.edu.tr; on leave from Physics Department, Baku State University, Baku, Azerbaijan.

and broadening of the phonon lines during heating are a manifestation of phonon-phonon interaction and the measurements of phonon frequency and line width as a function of temperature allow one to study the anharmonicity of the lattice vibrations.

The phonon spectra of $\text{GaS}_{0.25}\text{Se}_{0.75}$ layered crystals have been reported previously at room temperature from Raman [3, 4] and infrared [5] measurements. While much is known on the phonon spectra of $\text{GaS}_{0.25}\text{Se}_{0.75}$, temperature dependence of the phonon frequency and line width have not yet been studied. In our previous paper [6], we presented the temperature dependencies (10–300 K) of the Raman-active mode frequencies and line widths in $\text{GaS}_{0.5}\text{Se}_{0.5}$ layered crystal. It was shown that the observed softening and broadening of the optical phonon lines can be explained by the contributions from thermal expansion, lattice anharmonicity and crystal disorder.

The aim of the present work was to measure the frequency and line width of the zone-center optical modes in $\text{GaS}_{0.25}\text{Se}_{0.75}$ crystals from the Raman spectra in the 10–300 K temperature range and to compare the experimental results with the existing theories of anharmonicity of lattice vibrations in crystals.

2. Crystal symmetry and group-theoretical analysis

The $\text{GaS}_x\text{Se}_{1-x}$ mixed crystals, like binary compounds GaS and GaSe, have a layered structure. Each layer has four atomic planes with the sequence S(Se)–Ga–Ga–S(Se). Depending on the layer stacking kind, polytypes ε , β and γ are distinguished [7]. GaSe crystals grown from the melt by the Bridgman method present ε modification whereas GaS crystals invariably present β modification, which sometimes is also found in vapor-grown GaSe. At $x = 0.25$, the $\text{GaS}_x\text{Se}_{1-x}$ crystal is a mixture of the ε and β -polytypes [8].

The space groups of β -GaS and ε -GaSe crystals are D_{6h}^4 and D_{3h}^1 , respectively [3, 4]. In the β - and ε -type structures the primitive hexagonal unit cell consists of four formula units from two neighboring layers. For GaS, there are 24 normal modes of vibration at the center of the Brillouin zone and these can be described by the irreducible representations of the D_{6h} point group

$$\Gamma \equiv 2A_{1g} + 2A_{2u} + 2B_{1u} + 2B_{2g} + 2E_{1g} + 2E_{1u} + 2E_{2g} + 2E_{2u}.$$

Thus, there are six Raman-active modes ($2A_{1g} + 2E_{1g} + 2E_{2g}$) and two infrared-active modes ($E_{1u} + A_{2u}$).

For ε -polytype of GaSe, 24 normal modes are given by the irreducible representations of the D_{3h} point group

$$\Gamma \equiv 4A_1' + 4A_2'' + 4E' + 4E''.$$

In this case, there are eleven Raman-active modes ($4A_1' + 3E' + 4E''$) and six infrared-active modes ($3A_2'' + 3E'$). One of the Raman-active $3E'$ modes ($E'^{(2)}$) and acoustic mode $E'^{(1)}$ are counterparts of one of the six Davydov doublets. The

remaining ten Raman-active modes ($4A'_1 + 2E' + 4E''$) are components of five Davydov doublets [9].

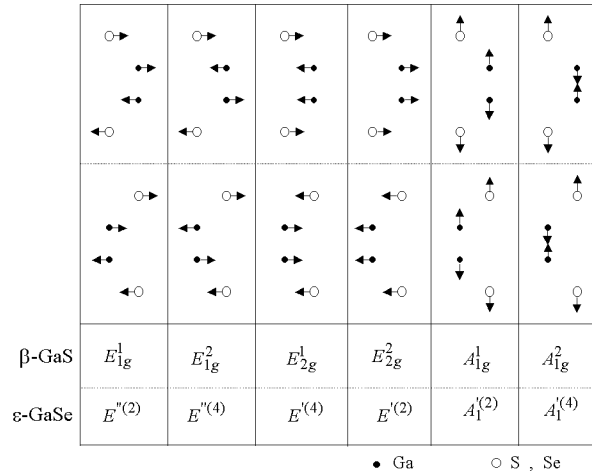


Fig. 1. Atomic displacement vectors for interlayer and intralayer Raman-active optical modes of β -GaS and ε -GaSe layered crystals.

The symmetry coordinates found by Melvin projection operator method were used to obtain the displacement vectors of atoms in all phonon modes of GaS and GaSe crystals. Figure 1 shows the atomic displacement vectors for Raman-active interlayer and intralayer modes. In these modes all the gallium and sulfur (selenium) atoms move either perpendicular or parallel to the layers.

3. Experimental details

$\text{GaS}_{0.25}\text{Se}_{0.75}$ single crystals were grown by the Bridgman method. The analysis of X-ray diffraction data showed that they crystallize in a hexagonal unit cell with parameters: $a = 0.3714$ and $c = 1.5890$ nm. Crystals suitable for measurements were obtained by easy cleaving perpendicular to optical c -axis. $\text{GaS}_{0.25}\text{Se}_{0.75}$ is a p -type semiconductor having an indirect band gap energies of 2.23 eV and 2.10 eV at 4.2 and 300 K, respectively [10].

Raman scattering measurements in $\text{GaS}_{0.25}\text{Se}_{0.75}$ layered crystal were performed in the backscattering geometry in the frequency range $10\text{--}360\text{ cm}^{-1}$. A 30 mW He-Ne laser (632.8 nm) was used as the exciting light source. The scattered light was analyzed using a Jobin Yvon U-1000 double grating spectrometer and a cooled GaAs photomultiplier supplied with the usual photon counting electronics. The Raman line positions were determined within an accuracy of $\pm 0.1\text{ cm}^{-1}$. A CTI-Cryogenics M-22 closed cycle helium cryostat was used to cool the crystals from room temperature down to 10 K. The temperature was controlled within an

accuracy of ± 0.5 K. In order to avoid sample-heating effects, we have chosen a cylindrical lens to focus the incident beam on the sample.

4. Results and discussion

Figure 2 represents the Raman spectra of $\text{GaS}_{0.25}\text{Se}_{0.75}$ crystal at 10 K. The insets of Fig. 2 show two extended individual parts of the spectra at 10 and 300 K. The shift and broadening of phonon lines with increasing temperature are seen. One-mode behavior of interlayer $E^{(2)}(E_{2g}^2)$ and intralayer $E^{(2)}(E_{1g}^1)$, $[E^{(4)}(\text{TO})](E_{2g}^1)$, $[E^{(4)}(\text{LO})](E_{2g}^1)$ shear modes, and two-mode behavior of intralayer $A_1^{(2)}(A_{1g}^1)$ and $A_1^{(4)}(A_{1g}^2)$ compressional modes are in agreement with that of Refs. [3, 4]. The room temperature frequency values of $\text{GaS}_{0.25}\text{Se}_{0.75}$ crystal were found to be 16.6 [$E^{(2)}(E_{2g}^2)$], 58.9 [$E^{(2)}(E_{1g}^1)$], 129.1 and 145.9 [$A_1^{(2)}(A_{1g}^1)$], 212.2 {[$E^{(4)}(\text{TO})](E_{2g}^1)$ }, 243.4 {[$E^{(4)}(\text{LO})](E_{2g}^1)$ }, 300.4 and 324.9 [$A_1^{(4)}(A_{1g}^2)$]. The interlayer shear mode $E^{(2)}(E_{2g}^2)$ is related to the weak layer-layer interaction for which entire layers vibrate rigidly out of phase with their neighbors (Fig. 1). The low value of this mode frequency ($\nu = 16.6 \text{ cm}^{-1}$) gives information about the strength of the layer-layer interaction in $\text{GaS}_{0.25}\text{Se}_{0.75}$. There is large difference between the mode Grüneisen parameters (γ) of the interlayer (22.7, 22.1) and intralayer (1.0–2.6, 1.3–3.9) modes of layered crystals GaS and GaSe, respectively [11, 12]. The difference in the mode Grüneisen parameters represents the difference in the interlayer and intralayer restoring forces. The frequency shifts of

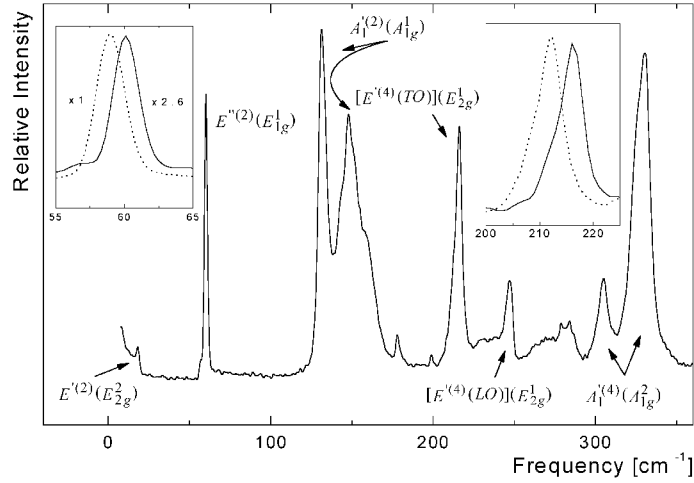


Fig. 2. Raman spectra of $\text{GaS}_{0.25}\text{Se}_{0.75}$ crystal at $T = 10$ K. Insets: comparison of the extended parts of Raman spectra at $T = 10$ K (solid curves) and $T = 300$ K (dashed curves).

$\text{GaS}_{0.25}\text{Se}_{0.75}$ Raman modes in the temperature range 10–300 K were found to be 1.5 [$E''^{(2)}(E_{2g}^2)$], 1.2 [$E''^{(2)}(E_{1g}^1)$], 2.4 and 2.2 [$A_1'^{(2)}(A_{1g}^1)$], 3.9 {[$E'^{(4)}(\text{TO})$](E_{2g}^1)}, 3.6 {[$E'^{(4)}(\text{LO})$](E_{2g}^1)}, 3.8 and 5.2 [$A_1'^{(4)}(A_{1g}^2)$].

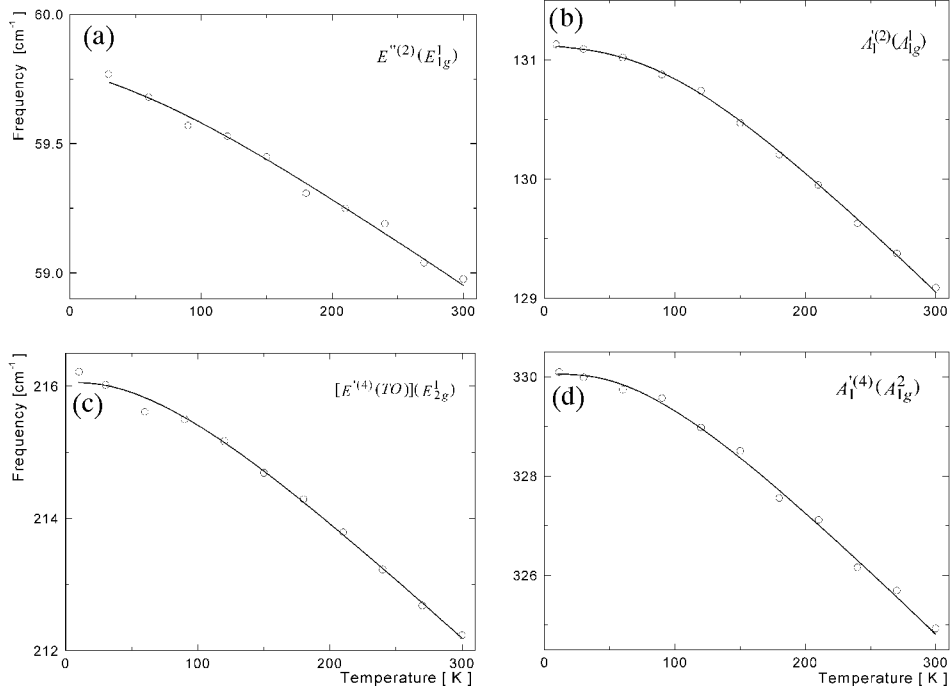


Fig. 3. Temperature dependencies of $E''^{(2)}(E_{1g}^1)$ (a), $A_1'^{(2)}(A_{1g}^1)$ (b), [$E'^{(4)}(\text{TO})$](E_{2g}^1) (c), and $A_1'^{(4)}(A_{1g}^2)$ (d) intralayer mode frequencies in $\text{GaS}_{0.25}\text{Se}_{0.75}$ crystal (open circles). The solid curves represent the theoretical fits using Eqs. (1)–(3).

Analysis of the temperature dependence of the frequency shift for the low-frequency interlayer mode $E'^{(2)}(E_{2g}^2)$ does not yield a physically meaningful decay channel. This is consistent with the narrow line width of this mode, which indicates a long lifetime. Figures 3a–d show the experimental results (open circles) for the line positions $\nu(T)$ of intralayer modes $E''^{(2)}(E_{1g}^1)$, $A_1'^{(2)}(A_{1g}^1)$, [$E'^{(4)}(\text{TO})$](E_{2g}^1), and $A_1'^{(4)}(A_{1g}^2)$ respectively. The phonon frequency shift with temperature can be described by the expression [13–15]

$$\nu(T) = \nu_0 + \Delta_1(T) + \Delta_2(T), \quad (1)$$

where $\nu_0 + \Delta_2(0)$ is the Raman frequency as T approaches 0 K, $\Delta_1(T)$ represents the volume dependence of the frequency due to the thermal expansion of the crystals and $\Delta_2(T)$ specifies the contribution of anharmonic coupling to phonons of other branches. $\Delta_1(T)$ can be written as

$$\Delta_1(T) = \nu_0 \left\{ \exp \left[-3\gamma \int_0^T \alpha(T') dT' \right] - 1 \right\}, \quad (2)$$

where $\alpha(T)$ is the coefficient of linear thermal expansion.

The purely anharmonic contribution to the frequency shift can be modeled as

$$\Delta_2(T) = A \left(1 + \frac{1}{e^{x_1} - 1} + \frac{1}{e^{x_2} - 1} \right), \quad (3)$$

which represents the optical phonon coupling to two different phonons (three-phonon processes). Here, $x_1 = hc\nu_1/k_B T$ and $x_2 = hc\nu_2/k_B T$. In the present study the experiments were carried out at temperatures below the Debye temperatures of GaS and GaSe crystals ($\theta_D = 425$ K [16] and 342 K [17], respectively). Thus, the three-phonon process is dominant and the higher-order processes can be neglected.

The frequency shifts for intralayer modes of $\text{GaS}_{0.25}\text{Se}_{0.75}$ crystal were fitted by means of Eqs. (1)–(3) using the experimental values of γ and $\alpha(T)$ for GaS and GaSe [11, 12, 18] with A , ν_0 , ν_1 , and ν_2 as adjustable parameters, keeping the sum, $\nu_1 + \nu_2 = \nu_0$, a constant (energy conservation). For all intralayer modes, the agreement between the theoretical and experimental dependencies was found to be good. Figure 3 shows this agreement for the intralayer modes $E''^{(2)}(E_{1g}^1)$, $A_1''^{(2)}(A_{1g}^1)$, $[E'^{(4)}(\text{TO})](E_{2g}^1)$, and $A_1'^{(4)}(A_{1g}^2)$. The resulting parameters for all the intralayer modes are shown in Table. Generally, to identify the decay channels of phonon modes, all possible interactions should be considered for the decay processes taking into account the phonon dispersion curves. Unfortunately, lack of phonon dispersion curves for $\text{GaS}_{0.25}\text{Se}_{0.75}$ does not allow for confirmation of decay channels determined by fitting Eqs. (1)–(3) to data.

TABLE
Parameters for fitting the temperature dependencies of Raman frequencies of $\text{GaS}_{0.25}\text{Se}_{0.75}$ crystal.

Modes	ν_0	ν_1	ν_2	A
	[cm ⁻¹]			
$E''^{(2)}(E_{1g}^1)$	59.8	39.8	20.0	-0.04
$A_1''^{(2)}(A_{1g}^1)$	131.1	87.0	44.1	+0.02
$A_1''^{(2)}(A_{1g}^1)$	147.3	94.5	52.8	+0.13
$[E'^{(4)}(\text{TO})](E_{2g}^1)$	216.7	144.7	72.0	-0.60
$[E'^{(4)}(\text{LO})](E_{2g}^1)$	247.2	164.3	82.9	-0.54
$A_1'^{(4)}(A_{1g}^2)$	305.4	204.1	101.3	-0.88
$A_1'^{(4)}(A_{1g}^2)$	331.7	220.9	110.8	-1.65

We have also calculated separately the thermal-expansion contribution [$\Delta_1(T)$] from Eq. (2) and the purely anharmonic contribution [$\Delta_2(T)$] from Eq. (3) to the line shift for intralayer modes of $\text{GaS}_{0.25}\text{Se}_{0.75}$ crystal by using the values of adjusted parameters A , ν_0 , ν_1 , and ν_2 obtained above. For the modes with low Grüneisen parameter ($\gamma \leq 2.0$) both contributions $\Delta_1(T)$ and $\Delta_2(T)$ are negative. For the mode having $\gamma = 3.5$, $\Delta_1(T)$ continues to be negative, but $\Delta_2(T)$ changes sign and becomes positive. The variations of $\Delta_1(T)$ and $\Delta_2(T)$ are given in Fig. 4 for the intralayer $A_1^{(2)}(A_{1g}^1)$ and $A_1^{(4)}(A_{1g}^2)$ modes together

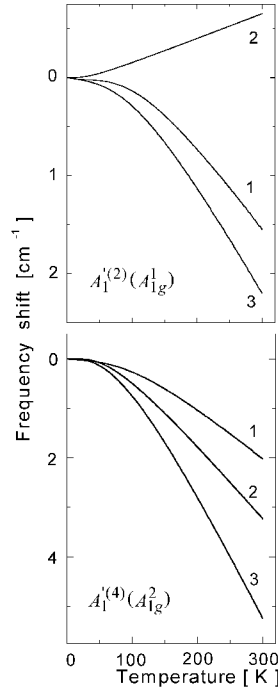


Fig. 4. Experimental Raman frequency shifts of $A_1^{(2)}(A_{1g}^1)$ and $A_1^{(4)}(A_{1g}^2)$ interlayer modes as a function of temperature (curves 3). Curves 1 and 2 represent the purely thermal expansion [$\Delta_1(T)$] and the purely anharmonic [$\Delta_2(T)$] contributions to the frequency shifts, respectively.

with the experimental frequency shifts. An interesting feature of these plots is that for $A_1^{(4)}(A_{1g}^2)$ mode with low value of Grüneisen parameter ($\gamma = 1.5$), the $\Delta_2(T)$ slightly prevails $\Delta_1(T)$, both being negative. However, for the $A_1^{(2)}(A_{1g}^1)$ mode with higher value of Grüneisen parameter ($\gamma = 3.5$), $\Delta_1(T)$ and $\Delta_2(T)$ have opposite signs. This may be associated with the difference in sets of atomic displacements for these modes. In the $A_1^{(4)}(A_{1g}^2)$ mode the restoring forces are due to the strong intralayer gallium-gallium ($C_{\text{Ga-Ga}} = 110$ and $C_{\text{Ga-Ga}} = 108$ N/m for

GaS [19] and GaSe [20], respectively) and gallium–sulfur (selenium) ($C_{\text{Ga-S}} = 130$ and $C_{\text{Ga-Se}} = 123$ N/m) and weak interlayer sulfur–sulfur (selenium–selenium) ($C_{\text{S-S}} = 9.5$ and $C_{\text{Se-Se}} = 9.2$ N/m) bonds (see Fig. 1). On the other hand, in the $A_1^{(2)}(A_{1g}^1)$ mode gallium–sulfur (selenium) bonds are not involved in the restoring forces. Here C is the compressional force constant associated with the relative displacements of the atomic planes.

The line width of the $\text{GaS}_{0.25}\text{Se}_{0.75}$ phonons were studied as a function of temperature in the range of 10–300 K. The line width of all optical modes are found to increase with temperature. The broadening of the phonon lines is due to anharmonicity of the lattice vibrations. The presence of anharmonic forces in a crystal leads to interactions between the harmonic normal modes. These interactions produce a temperature dependent lifetime of the normal modes.

The temperature dependence of the phonon line width can be described as follows [13, 15, 21, 22]:

$$\Gamma = \Gamma_0 + C^* \left(1 + \frac{1}{e^{x_1} - 1} + \frac{1}{e^{x_2} - 1} \right), \quad (4)$$

where Γ_0 is the temperature-independent broadening due to the disorder of crystal, C^* is the broadening of the phonon line due to the cubic anharmonicity at absolute zero (the decrease in phonon lifetime τ due to the decay of the optical phonon into two different phonons).

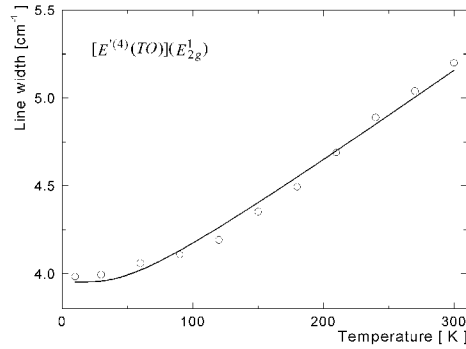


Fig. 5. Temperature dependence of $[E^{(4)}(\text{TO})](E_{2g}^1)$ intralayer mode line width (open circles). The solid curve represents the theoretical fit using Eq. (4).

The experimental data of phonon line width for intralayer modes of $\text{GaS}_{0.25}\text{Se}_{0.75}$ crystal were fitted by means of Eq. (4) with Γ_0 , C^* , ν_1 , and ν_2 as fitting parameters, keeping the sum of $\nu_1 + \nu_2 = \nu_0$ constant. We obtained quantitative agreement between calculated curves and experimental points for all intralayer modes. Figure 5 represents the line width broadening for the intralayer $[E^{(4)}(\text{TO})](E_{2g}^1)$ mode versus temperature. The fitting parameters Γ_0 , C^* , ν_1 , and ν_2 are found to be 3.5, 0.4, 144.7, and 72.0 cm^{-1} , respectively. It is worth

noting that line broadening of $[E^{(4)}(\text{TO})](E_{2g}^1)$ mode due to crystal disorder ($\Gamma_0 = 3.5 \text{ cm}^{-1}$) is less than that for the corresponding mode in $\text{GaS}_{0.5}\text{Se}_{0.5}$ crystal ($\Gamma_0 = 6.9 \text{ cm}^{-1}$) [6], as expected.

5. Conclusions

The Raman line shift and broadening of intralayer modes in $\text{GaS}_{0.25}\text{Se}_{0.75}$ crystal with temperature is well described by purely anharmonic (phonon–phonon coupling) and purely volume (thermal expansion) contributions. The cubic (three-phonon) processes with energy conservation is responsible for the purely anharmonic contributions to the softening and broadening of the intralayer phonon lines. The broadening of the phonon lines due to inherent disorder nature of the crystal is estimated.

Acknowledgment

We would like to thank R. Pala for his assistance.

References

- [1] A. Masui, S. Onari, K. Allakhverdiev, F. Gashimzade, T. Mamedov, *Phys. Status Solidi B* **223**, 139 (2001).
- [2] M.A. Osman, *Physica B* **275**, 351 (2000).
- [3] A. Mercier, J.P. Voitchovsky, *Solid State Commun.* **14**, 757 (1974).
- [4] M. Hayek, O. Brafman, R.M.A. Lieth, *Phys. Rev. B* **8**, 2772 (1973).
- [5] V. Riede, H. Neumann, H. Sobotta, F. Levy, *Solid State Commun.* **34**, 229 (1980).
- [6] N.M. Gasanly, A. Aydinli, C. Kocabas, H. Ozkan, *Phys. Scr.* **65**, 534 (2002).
- [7] A. Kuhn, A. Chevy, R. Chevalier, *Phys. Status Solidi A* **31**, 469 (1975).
- [8] G.B. Abdullaev, K.R. Allakhverdiev, R.Kh. Nani, E.Yu. Salaev, M.M. Tagyev, *Phys. Status Solidi A* **53**, 549 (1979).
- [9] H. Yoshida, S. Nakashima, A. Mitsuishi, *Phys. Status Solidi B* **59**, 655 (1973).
- [10] A. Mercier, J.P. Voitchovsky, *J. Phys. Chem. Solids* **36**, 1411 (1975).
- [11] A. Polian, J.C. Chervin, J.M. Besson, *Phys. Rev. B* **22**, 3049 (1980).
- [12] M. Gauthier, A. Polian, J.M. Besson, A. Chevy, *Phys. Rev. B* **40**, 3837 (1989).
- [13] J. Menendez, M. Cardona, *Phys. Rev. B* **29**, 2051 (1984).
- [14] A. Debernardi, *Phys. Rev. B* **57**, 12847 (1998).
- [15] A. Debernardi, *Solid State Commun.* **113**, 1 (2000).
- [16] B.M. Powell, S. Jandl, J.L. Brebner, F. Levy, *J. Phys. C, Solid State Phys.* **10**, 3039 (1977).
- [17] S. Jandl, J.L. Brebner, B.M. Powell, *Phys. Rev. B* **13**, 686 (1976).

- [18] G.L. Belenkii, R.A. Suleymanov, N.A. Abdullaev, V.Ya. Shteinsraiber, *Sov. Phys.-Solid State* **26**, 2142 (1984).
- [19] G. Lucazeau, *Solid State Commun.* **18**, 917 (1976).
- [20] T.J. Wieting, *Solid State Commun.* **12**, 931 (1973).
- [21] A. Debernardi, M. Cardona, *Physica B* **263-264**, 687 (1999).
- [22] S. Anand, P. Verma, K.P. Jain, S.C. Abbi, *Physica B* **226**, 331 (1996).